BEILSTEIN JOURNAL OF NANOTECHNOLOGY

Size control of high-molecular-weight polylactide nanoparticles by nanoprecipitation

Vladislav Potseleev[1,2], Artem Kondratenko[3], Eugene Statnik[4,5], Anna Druzina[6] and Sergey Uspenskii[*1,2]

Full Research Paper

Open Access

Address:
[1]Enikolopov Institute of Synthetic Polymeric Materials, Russian Academy of Sciences, 70 Profsoyuznaya St., Moscow 117393, Russia, [2]Martin'ex International Research and Development Centre, 12 2nd Vladimirskaya St., Moscow 111123, Russia, [3]Mendeleev University of Chemical Technology of Russia, 9 Miusskaya Square, Moscow 125047, Russia, [4]NUST MISIS, 4 Leninsky Prospekt, Moscow 119049, Russia, [5]Center for Engineering Systems and Sciences, Bolshoy Boulevard 30, Building 1, Moscow 121205, Russia and [6]A. N. Nesmeyanov Institute of Organoelement Compounds, Russian Academy of Sciences, 28 Vavilova St., Moscow 119334, Russia

Email:
Sergey Uspenskii[*] - uspenskii@ispm.ru

* Corresponding author

Keywords:
acetonitrile; nanoparticle; nanoprecipitation; PLGA; polylactide; poly(lactide-*co*-glycolide)

Beilstein J. Nanotechnol. **2026,** *17,* 1624–1635.
https://doi.org/10.3762/bjnano.17.111

Received: 01 September 2026
Accepted: 05 November 2026
Published: 17 November 2026

Associate Editor: J. J. Schneider



© 2026 Potseleev et al.; licensee Beilstein-Institut.
License and terms: see end of document.

Abstract

Particle size is a central formulation variable for polymeric nanocarriers intended for delivery applications. In this study, polylactide (PLA) and poly(lactide-*co*-glycolide) nanoparticles were prepared by nanoprecipitation, and the particle size was examined as a function of polymer molecular weight, organic solvent, polymer concentration, organic-phase fraction, and stabilizer. In water-miscible solvents, the PLA particle diameter generally increased with molecular weight, but the magnitude of the increase depended on the solvent. Acetonitrile produced 79 ± 10 nm particles from 111 kDa PLA, whereas 1,4-dioxane restrained the size increase from 170 kDa upwards. Reducing the concentration of 170 kDa PLA in acetonitrile from 1 to 0.0625 wt % decreased the hydrodynamic diameter from 120 ± 8 to 58 ± 4 nm. At a fixed PLA molecular weight (170 kDa), the measured diameter depended strongly on the stabilizer and ranged from 79 ± 12 nm with Tween 80 to 180 ± 20 nm with sodium dodecyl sulfate. By contrast, ethyl acetate produced micrometer-scale PLA particles spanning approximately 1–10 μm. The dispersions characterized in detail were narrowly distributed (PDI 0.08–0.16) and negatively charged (zeta potential from −12 to −16 mV); scanning electron microscopy confirmed a regular spherical morphology. These results define the conditions under which high-molecular-weight PLA can be brought into the sub-100 nm range targeted for carriers in neutron capture therapy.

Introduction

The steadily growing incidence of cancer calls for the development of new, more effective methods of prevention and therapy. Research efforts are therefore directed toward the design of new antitumor agents that act selectively on tumor cells with minimal damage to healthy cells and tissues. Neutron capture therapy (NCT) is a promising method in oncology, relying on the selective accumulation of stable isotopes (e.g., ^{10}B, ^{6}Li, or ^{157}Gd) with high neutron capture cross sections in tumor tissue, followed by localized irradiation [1]. NCT therefore requires biocompatible nanoparticles that carry a large number of boron, lithium, or gadolinium atoms and accumulate selectively in malignant cells [2,3]. One promising approach to the targeted delivery of drugs to cancer cells is the use of colloidal drug forms based on polymeric nanoparticles (NPs, including nanospheres and nanocapsules) [4,5]. The primary advantage of such systems lies in their ability to overcome biological barriers, enabling targeted delivery of active substances. This is made possible by the tunable surface properties of polymeric NPs, controlled biodegradation rates, and their versatility in encapsulating both hydrophilic and hydrophobic compounds [6-9]. The key advantage of NCT is the lack of need for prolonged drug release, as the therapeutic effect is achieved in a single session lasting a few hours [10]. Accordingly, the requirements placed on the release profile are relaxed, and the polymer matrix is required primarily to deliver the isotope to the tumor and to retain it there during the irradiation session. However, to ensure stability and extend the shelf life of drugs, nanoparticles based on biocompatible polymers such as polylactide (PLA) [11], which exhibit high resistance to hydrolysis, are preferred. This simplifies their clinical application compared to less stable analogs like poly(lactide-*co*-glycolide) (PLGA) and is consistent with the strategy of stimulus-induced release [12-14].

A critical factor determining the efficacy of nanoparticles as carriers for targeted delivery of therapeutic agents is their size. Particles in the 10–100 nm range possess unique pharmacokinetic properties as their size is optimal for overcoming two critical barriers: They are large enough to avoid rapid renal elimination (typical for particles <10 nm) but small enough (<100 nm) to effectively penetrate and accumulate in tumor tissue via the enhanced permeability and retention effect [15,16]. Within this window, the efficiency of cellular uptake is itself size-dependent and is commonly reported to pass through a maximum at about 30–60 nm [17]. Understanding which parameters control particle size, and how the smallest possible size can be achieved, is therefore of key importance since tissue penetration, cellular uptake, and circulation behavior of the carrier are all governed by this parameter.

Despite extensive research on methods for synthesizing polymeric nanoparticles [18,19], the reproducible preparation of sub-100 nm particles from high-molecular-weight PLA remains challenging. A systematic analysis of literature data, summarized in Table 1, indicates that standard approaches, such as nanoprecipitation and emulsion evaporation, have been successfully employed to produce nanoparticles from various polymers, including poly(methyl methacrylate) (PMMA), polycaprolactone (PCL), and PLGA copolymers. However, these systems typically yield particles ranging from 50 to several hundred nanometers, consistent with the typical sizes achieved by these methods [20-38]. Notably, the use of high-molecular-weight PLA, which exhibits enhanced hydrolytic stability, introduces additional technological challenges that further increase the average particle size [39-42]. The few reports of PLA particles at or below 100 nm refer to oligomeric or low-molecular-weight grades. In Table 1, a 16 kDa PLA gives 101 ± 3 nm, whereas raising the molecular weight to 209 kDa under otherwise identical conditions already yields 138 ± 2 nm [39]; the 1000 kDa entry reaching 112 ± 18 nm was obtained from dichloromethane (DCM) by an emulsion route rather than by nanoprecipitation [41]. The range of the order of 10^2 kDa, which is the one relevant for hydrolytically stable matrices, is therefore precisely the range in which the sub-100 nm target has not been met. This limitation restricts the potential applications of such systems in fields requiring ultrasmall sizes, such as NCT.

The aim of the present study was therefore to investigate and optimize the parameters governing the nanoprecipitation-based synthesis of PLA and PLGA nanoparticles (solvent type, polymer molecular weight, polymer concentration, and nature and concentration of the surfactant) in order to establish reliable conditions for obtaining ultrasmall, uniform PLA nanoparticles in the sub-100 nm range from high-molecular-weight polymers. The synthesis routes and structure–size relationships established here are intended as a basis for future work on the encapsulation of boron-containing compounds into PLA nanoparticles, with a view toward the development of boron-containing nanocarriers for NCT of cancer.

Results and Discussion

Influence of synthesis parameters on nanoparticle size

Nanoprecipitation [43,44] was selected as the baseline method. In this process, the polymer solution is diluted past its solubility limit within the time of mixing, and particles form by homogeneous nucleation followed by growth and arrested coalescence inside the transient solvent-rich zone that surrounds the incoming stream; the underlying mechanism is the so-called

Table 1: Influence of polymer type, molecular weight, solvent, concentration, and surfactant on the size of nanoparticles as characterized by DLS, SEM, and TEM.[a]

Polymer	Molecular weight, kDa	Solvent	Concentration, %	Surfactant	Size, nm	Characterization method	Reference
polystyrene	N/A	ethyl acetate	1	PVA	381 ± 20	DLS	[20]
			5		502 ± 25		
			10		666 ± 30		
	25	THF	0.4	—	250 ± 3	DLS	[21]
				CTAB	160 ± 1		
		DMA		—	560 ± 8		
PMMA	11	acetone	0.4	—	310	SEM	[22]
					480	DLS	
	8	acetone	0.1	—	74 ± 5	DLS	[23]
		THF			100 ± 20		
chitosan	<100	acetic acid	0.5	lecithin	148 ± 29	DLS	[24]
	400		1	Span 80	510 ± 50	DLS	[25]
	700		1.5	Tween 60	300	SEM	[26]
alginate	100	isooctane and 1-hexanol	0.5	CTAB	223 ± 82	DLS	[27]
			1		343 ± 75		
			2		440 ± 151		
	N/A	water	0.05	AOT	139 ± 13	DLS	[28]
					60	SEM	
	N/A	water	1	PGPR	1000	SEM	[29]
PCL	14	acetone	0.4	PVA	152 ± 10	DLS	[30]
					258 ± 22		
	14	DCM	8	PVA	235	DLS	[31]
			20	PVA	364		
	14	DCM	5	PVA	202 ± 2	DLS	[32]
					149 ± 14	TEM	
	65	DCM	5	PVA	369 ± 3	DLS	[33]
PLGA75	40-75	acetone	1	Pluronic F127	180 ± 33	DLS	[34]
					172 ± 49	TEM	
	75	ethyl acetate	2	PVA	200	DLS	[35]
	12	benzyl alcohol	5	PVP	175	DLS	
PLGA50	30	acetonitrile	0.1	PVA	50	DLS	[36]
	40	acetonitrile	1	PVP	157 ± 2	DLS	[37]
	40	DCM	10	Tween 80	209 ± 16	DLS	[38]
PLA	16	acetone	0.375	Tween 80	101 ± 3	DLS	[39]
	209	acetone	0.375	Tween 80	138 ± 2	DLS	
	1000	DCM	1	Tween 20	112 ± 18	SEM	[41]
	31.3	DCM	2	PVA	345 ± 16	DLS	[42]

[a]PVA: polyvinyl alcohol; THF: tetrahydrofuran; CTAB: cetyltrimethylammoniumbromid; DMA: dimethylacetamide; AOT: bis(2-ethylhexyl) sulfosuccinate sodium salt; PGPR: polyglycerol polyricinoleate; DCM: dichloromethane; PVP: polyvinylpyrrolidone.

Ouzo effect [45,46]. We then examined the key factors that govern the size of the PLA nanoparticles, using polylactides with molecular weights of 44, 111, 170, 330, and 442 kDa. PLGA50/50 was employed as a reference polymer due to its well-documented ability to form smaller particles. The 50:50 lactide-to-glycolide copolymer was chosen because its glycolic acid units make it the most hydrophilic member of the PLGA family. It therefore provides the greatest contrast to the more hydrophobic PLA and serves as a convenient reference against which the effect of polymer hydrophobicity on particle size can be judged. Since PLGA50/50 is not commercially available at the very high molecular weights of the highest PLA grades, samples of 41, 94, and 178 kDa were chosen to match the PLA series as closely as possible.

Influence of fully water-miscible solvents and polymer molecular weight

One of the most critical parameters affecting particle size is the choice of the solvent. The solvent must be miscible with water and capable of dissolving the polymer, while also influencing the rate of polymer precipitation and the stability of the resulting nanoparticles. Among the water-miscible solvents that dissolve polylactide, the most commonly used are tetrahydrofuran (THF), dioxane, acetonitrile, and acetone [47]. These four solvents were compared here for their ability to produce nanoparticles of controlled size and morphology, using both PLA and PLGA.

In all four solvents the average particle size increased with polymer molecular weight. This is because higher-molecular-weight PLA has longer chains, which are more prone to overlap and entanglement and form larger aggregates during precipitation. Regarding the lower molecular weights, the smallest particles were obtained using acetonitrile, which is attributed to its favorable interaction with the polymer and its ability to facilitate rapid and uniform precipitation. Polylactide with a molecular weight of 111 kDa yielded particles approximately 80 nm in size (79 ± 10 nm) when acetonitrile was used as the solvent (Figure 1). At 170 kDa, the diameters obtained from acetonitrile and 1,4-dioxane already coincide within the experimental scatter; at higher molecular weights, the curves for the individual solvents diverge, dioxane restraining the growth of the particles more effectively (Figure 1). Acetonitrile is therefore the solvent of choice when ultrasmall and homogeneous particles are required from polymers of the lower molecular weights studied, whereas 1,4-dioxane becomes preferable from about 170 kDa upwards. This agrees with the literature data in Table 1, where acetonitrile gave smaller PLGA particles (e.g., 50 nm for 30 kDa PLGA [36]). It is also consistent with the observation that the choice of solvent shifts the boundaries of the Ouzo effect region, and hence the accessible particle size, far more strongly than solvent polarity alone would suggest [48]. The molecular weights covered here lie well above those for which sub-100 nm PLA particles have previously been reported (Table 1), so that already the 79 ± 10 nm obtained from 111 kDa PLA falls outside the range covered by the literature.

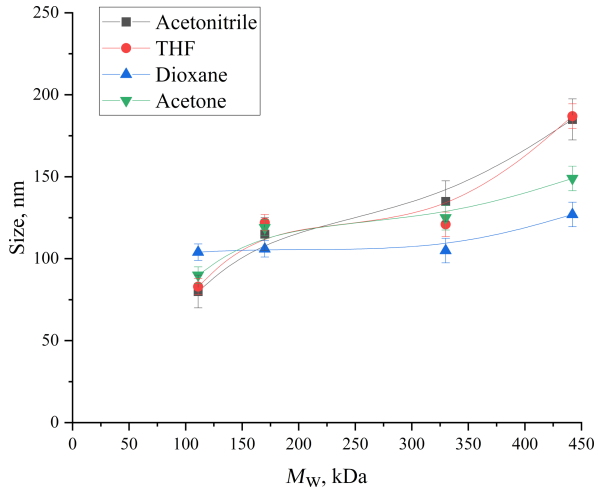


Figure 1: Dependence of PLA nanoparticle size obtained by nanoprecipitation on molecular weight (solvents: acetonitrile, acetone, dioxane, THF). The lines are guides to the eye.

A similar trend was observed for PLGA50/50, where the average particle size also strongly depended on the polymer molecular weight. Specifically, for molecular weights below 100 kDa, smaller particles with sizes ranging from 50 to 60 nm were obtained (Table 2).

All of the nanoparticles had a regular spherical morphology with a smooth surface and a narrow size distribution. This is illustrated by the representative SEM image and the corresponding particle size distribution histogram for PLGA50/50 nanoparticles with M_w = 94 kDa (Figure 2).

Table 2: Size of PLA and PLGA50/50 nanoparticles obtained by nanoprecipitation in acetonitrile as a function of polymer molecular weight (1 wt % polymer, 1 wt % polyvinyl alcohol, organic-phase fraction 10 vol %).

Polymer	Molecular weight, kDa	Size, nm	PDI	Zeta potential, mV
PLA	44	73 ± 10	0.11 ± 0.02	−12.3 ± 1.8
PLA	111	79 ± 10	0.12 ± 0.02	−13.1 ± 2.0
PLA	170	120 ± 8	0.15 ± 0.03	−13.8 ± 2.1
PLA	330	132 ± 15	0.14 ± 0.03	−13.4 ± 2.0
PLA	442	186 ± 16	0.16 ± 0.03	−14.6 ± 2.3
PLGA50/50	41	55 ± 4	0.08 ± 0.02	−15.8 ± 1.7
PLGA50/50	94	57 ± 5	0.08 ± 0.02	−15.2 ± 1.8
PLGA50/50	178	109 ± 7	0.14 ± 0.03	−16.4 ± 2.2

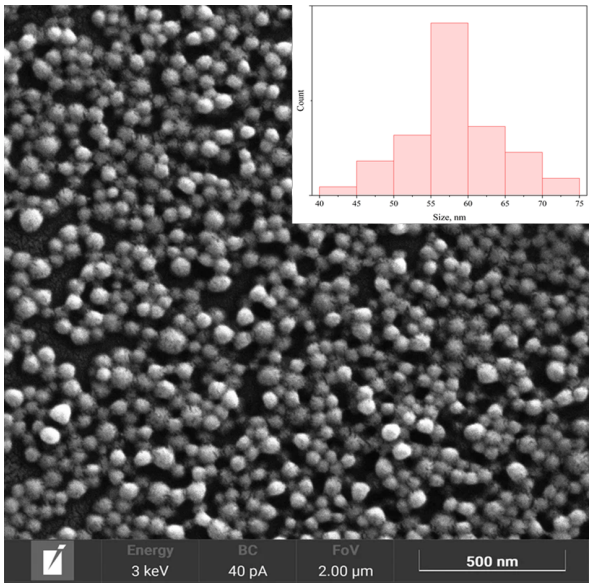


Figure 2: Representative scanning electron micrograph of PLGA50/50 nanoparticles with M_w = 94 kDa obtained by nanoprecipitation in acetonitrile; the inset shows the corresponding particle size distribution histogram (n = 200 particles).

Influence of a partially water-miscible solvent on nanoparticle size and morphology

Polymer particles can also be produced using solvents with limited water miscibility. Ethyl acetate is a representative example of such solvents; its solubility in water is limited to approximately 8 wt % [49]. In this case, the method occupies an intermediate position between classical nanoprecipitation and conventional emulsion techniques. Literature data indicate that PLGA50/50 particles prepared by similar approaches using ethyl acetate typically form nanoparticles ranging from 40 to 400 nm, depending on the stabilizer and process parameters [50].

As shown in Figure 3, the PLA particles obtained by this method were broadly distributed over the range from 1 to 10 µm, the greater part of the population lying between 3 and 9 µm. Since ethyl acetate is only partially miscible with water, it diffuses much more slowly from the forming polymer solution droplets into the aqueous phase compared to fully water-miscible solvents such as acetone, THF, or acetonitrile. This slower solvent displacement leads to the formation of significantly larger initial droplets that solidify into microparticles. In this solvent, the final size is therefore governed by the energy supplied during dispersion rather than by spontaneous emulsification [51]. All preparations reported in this work were carried out under identical low-shear conditions (magnetic stirring), so that the comparison made here is one of solvents at constant energy input: Under these conditions acetonitrile, acetone, THF, and dioxane form nanoparticles spontaneously, whereas ethyl acetate does not.

In contrast to PLGA50/50, which typically yields nanoparticles in the range of 40–400 nm even when ethyl acetate is used [50], high-molecular-weight PLA produces much larger particles under identical conditions. This pronounced difference is mainly due to the higher hydrophobicity of PLA compared to PLGA50/50. Because PLA is more hydrophobic, polymer precipitation occurs more slowly upon contact with the aqueous phase. As a result, the larger droplets persist longer and solidify before they can shrink or break up significantly.

In summary, both the water miscibility of the organic solvent and the polymer molecular weight exert a strong influence on the size of PLA particles obtained by nanoprecipitation. Among fully water-miscible solvents, acetonitrile proved to be the most advantageous at the lower molecular weights, enabling the formation of ultrasmall nanoparticles as small as 58 nm at a reduced polymer concentration, whereas from about 170 kDa upwards, 1,4-dioxane limited the growth of the particles more effectively. In contrast, the partially water-miscible ethyl acetate leads to significantly larger microparticles (1–10 µm). This pronounced difference arises primarily from the slower diffusion of ethyl acetate into the aqueous phase combined with the higher hydrophobicity of PLA relative to PLGA50/50.

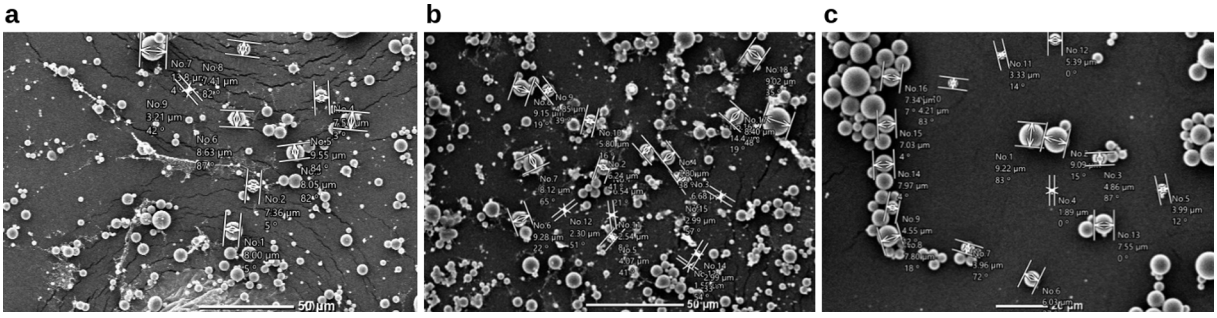


Figure 3: PLA 111 kDa (a), PLA 170 kDa (b), and PLA 442 kDa (c) particles obtained using ethyl acetate as the solvent.

Highly water-miscible solvents, particularly acetonitrile, are therefore essential for producing sub-100 nm PLA nanoparticles suitable for potential NCT applications. At the same time, partially water-miscible solvents such as ethyl acetate are more appropriate for fabricating larger microparticles intended for other biomedical applications (e.g., tissue engineering scaffolds or injectable formulations) [52].

Influence of polymer concentration and organic-to-aqueous phase ratio

The polymer concentration in the solution was also found to strongly affect the size of the resulting particles (Figure 4a). For instance, when producing PLA particles with a fixed molecular weight of 170 kDa, using the same solvent (e.g., acetonitrile), but increasing the concentration of polylactide from 0.0625% to 1%, the size of the nanoparticles increased from 58 to 120 nm. This substantial change in particle size with increasing polymer concentration can be attributed to the higher density of polymer chains in the solution, which leads to the formation of larger aggregates during the nanoprecipitation process. As the polymer concentration rises, the likelihood of intermolecular interactions and entanglement between polymer chains also increases, resulting in the formation of larger nanoparticles. A similar dependence of particle size on polymer concentration has been reported for PLGA50/50 (Table 1): As the concentration increased from 0.1% [36] to 10% [38], the reported size increased from 50 to 209 nm, although these literature data were obtained by different preparation methods.

However, under comparable synthesis conditions and at the same polymer concentration, PLGA tends to form somewhat smaller particles than PLA. This is due to the lower intrinsic viscosity and higher hydrophilicity of PLGA, which facilitate finer dispersion during nanoprecipitation. Nevertheless, this approach enables the production of nanoparticles smaller than 60 nm even from high-molecular-weight PLA, indicating that the nanoprecipitation method is applicable to both polymer systems.

In contrast, the volume ratio of the organic and aqueous phases was found to have almost no effect on the size of the resulting particles. When using a 1% polylactide solution, the particle size remained unchanged within the experimental scatter (110–120 nm) regardless of the proportion of the organic phase over the range studied (10–50 vol %, Figure 4b). Within the range tested, therefore, the volume ratio of the two phases does not determine the final size of the nanoparticles. The insensitivity of particle size to the phase volume ratio is advantageous from a practical standpoint, as it allows for greater flexibility in upscaling the production process without the need to precisely control this parameter. Read together with the concentration series, this result identifies which concentration actually controls the size. Raising the organic fraction from 10 to 50 vol % increases the total amount of polymer introduced into the system five-fold, and its mean concentration in the final mixture about four-fold, yet leaves the diameter unchanged; a comparable change of the concentration within the organic phase, by contrast, changes the diameter by a factor of about 1.5. The governing variable is therefore the concentration inside the injected polymer solution, before mixing, and not the mean concentration of the system after mixing. This is what would be expected if nucleation and growth are completed within the transient solvent-rich zone that forms around the incoming stream, the local composition of which is set by the composi-

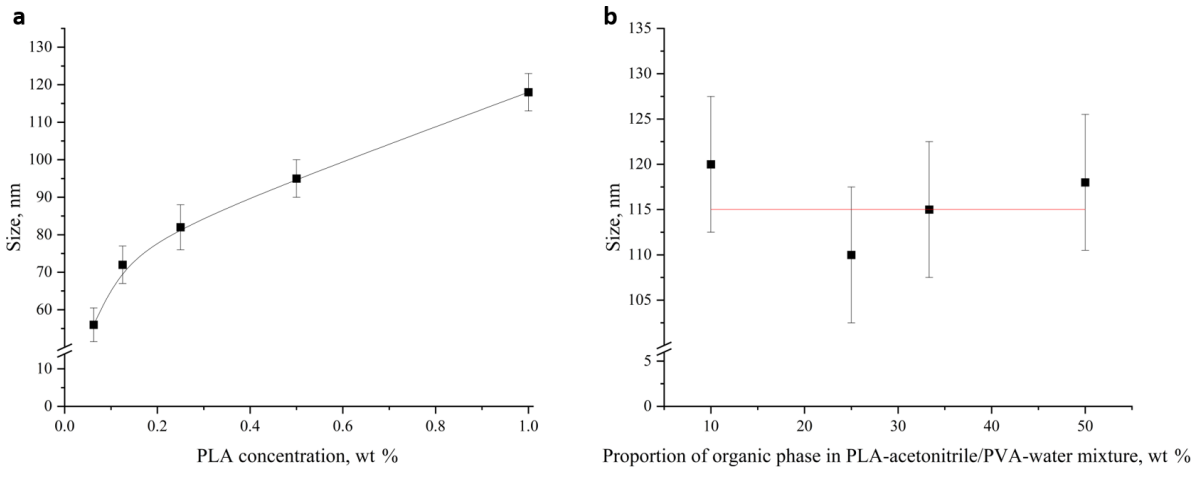


Figure 4: Dependence of PLA 170 kDa nanoparticle size obtained by nanoprecipitation on polymer concentration (a) and on the proportion of the organic phase, expressed relative to the volume of the aqueous phase (b).

tion of that stream. The subsequent dilution then determines how many particles are produced, but not how large each of them becomes. The two variables are consequently decoupled, and the practical consequence is that the amount of polymer processed per batch can be raised up to five-fold by increasing the organic fraction at constant particle size, provided that the polymer concentration within the organic phase is not raised at the same time. At the upper end of the range, the mixed solvent contains 50 vol % acetonitrile and is a considerably weaker non-solvent for PLA than at 10 vol %; that the size is nevertheless unchanged indicates that precipitation remains fast on the timescale of mixing throughout the range studied.

Notably, this behavior differs from that reported for PLGA-based systems. PLGA50/50 nanoparticles exhibit a pronounced dependence on the organic-to-aqueous phase ratio when prepared by the emulsion-solvent evaporation method. For instance, Hernández-Giottonini et al. [40] demonstrated that increasing the aqueous phase proportion from a 1:1 to a 1:3 organic-to-aqueous ratio resulted in a progressive decrease in particle size from 245 ± 12 nm to 159 ± 2 nm for PLGA50/50 using dichloromethane. In the same study, however, nanoprecipitation of that polymer from the fully water-miscible acetonitrile showed a much weaker dependence, the size varying only from 174.0 ± 0.3 to 156.6 ± 5.5 nm on changing the ratio from about 1:5 to 1:1; with ethyl acetate, a 1:4 ratio gave 176 ± 36 nm. This difference in behavior between the two methods is attributed to the more efficient dispersion of the organic phase at higher aqueous phase volumes in emulsion systems, leading to smaller emulsion droplets and finer particles. The contrasting insensitivity observed for high-molecular-weight PLA in the present study (nanoprecipitation) may stem from its higher solution viscosity and slower solvent diffusion kinetics, which dominate the precipitation process and largely override the influence of the phase volume ratio under the tested conditions.

The morphology of the PLA nanoparticles obtained under the optimized conditions is shown in Figure 5. The particles are spherical, isolated and narrowly distributed, and manual sizing gives a number-average diameter of 50–55 nm, somewhat below the hydrodynamic diameter measured by DLS.

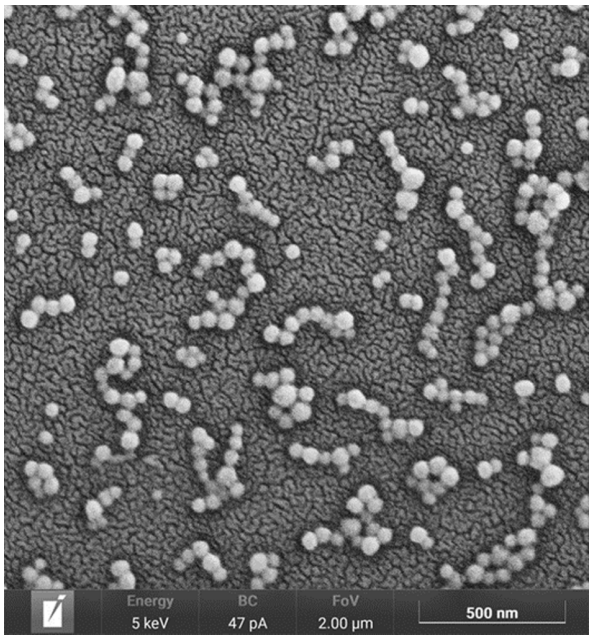


Figure 5: Scanning electron micrograph of PLA nanoparticles obtained by nanoprecipitation from a 0.0625 wt % solution of PLA (170 kDa) in acetonitrile with 1 wt % polyvinyl alcohol as stabilizer.

Influence of surfactant type and concentration

The type of surfactant plays a critical role in determining nanoparticle size as it governs emulsion stability and interfacial interactions between the organic and aqueous phases. In this study, surfactants with different hydrophilic–lipophilic balance (HLB) values were investigated, and the experimental data obtained under varying synthesis parameters are summarized in Table 3. All other synthesis parameters (polymer molecular weight, polymer concentration, solvent type, and organic-to-aqueous phase ratio) were kept constant.

Polyvinyl alcohol (PVA), commonly used for stabilizing PLA particles, typically produces particles of about 130 nm [53]. Pluronic F-127 (polyethylene oxide–polypropylene oxide–polyethylene oxide triblock copolymer, 12.7 kDa) enables the formation of smaller nanoparticles due to its lower molecular weight and faster adsorption kinetics, which improve stabilization of emulsion droplets [54]. Even smaller particles (≈80 nm) can be obtained using Tween 80 (HLB = 15) [55], whereas the use of the highly hydrophilic anionic surfactant sodium dodecyl sulfate (SDS, HLB = 40 on the Davies scale, which is not directly comparable with the Griffin values quoted for the non-ionic surfactants above) results in more than a twofold increase in particle size compared to Tween 80 [56,57]. In addition to surfactant type, its concentration also significantly affects particle size, with increasing concentration generally leading to larger particles.

Consistent with these trends, our experimental results (Table 3) demonstrate that nanoparticle size depends strongly on both formulation parameters and polymer properties. At a constant polymer and stabilizer concentration (1% PVA), increasing the molecular weight of PLA from 111 to 442 kDa leads to an increase in particle diameter from 79 to 186 nm. The choice of

Table 3: Size of PLA and PLGA50/50 nanoparticles obtained by nanoprecipitation in acetonitrile as a function of polymer molecular weight, polymer concentration, and the type and concentration of the surfactant.[a]

Polymer	M_w, kDa	Polymer concentration	Surfactant	Surfactant concentration	Size, nm
PLA	111	1%	PVA	1%	79 ± 10
	170				120 ± 8
	330				132 ± 15
	442				186 ± 16
PLA	170	1%	Tween 80	1%	79 ± 12
			Pluronic F-127		111 ± 10
			SDS		180 ± 20
PLA	170	0.5%	PVA	1%	96 ± 6
		0.25%			81 ± 5
		0.125%			72 ± 6
		0.0625%			58 ± 4
PLA	170	1%	PVA	1%	120 ± 8
				0.5%	119 ± 8
				0.1%	83 ± 5
				0.01%	86 ± 6
				0%	82 ± 5
PLGA50/50	41	1%	PVA	1%	55 ± 4
	94				57 ± 5
	178				109 ± 7

[a]PVA: polyvinyl alcohol; SDS: sodium dodecyl sulfate.

surfactant has a comparable impact: For PLA with M_w = 170 kDa, Tween 80 yields particles of 79 nm, whereas Pluronic F-127 gives 111 nm, PVA 120 nm, and SDS 180 nm. Polymer concentration is another key parameter; decreasing the concentration of 170 kDa PLA from 1% to 0.0625% reduces particle size from 120 to 58 nm. In contrast, varying PVA concentration from 0% to 1% shifts the size over a narrower interval, from 82 to 120 nm, and the change is not gradual. At and below 0.1 wt % PVA, the diameter is 82–86 nm, at and above 0.5 wt % it is 119–120 nm, and the transition occurs between these two levels. In the absence of a stabilizer the particles formed are initially the smallest, but such dispersions aggregate and sediment rapidly, so PVA was retained in the optimized formulation. Under similar conditions, PLGA (41–94 kDa) forms smaller particles (55–57 nm) than PLA of comparable molecular weight (although the two PLGA samples do not differ from one another beyond the experimental error), which highlights the difficulty of producing ultrasmall particles from high-molecular-weight PLA. Although the literature data in Table 1 report minimum sizes of ≈50 nm for PLGA, our results show that particles as small as 58 nm can be achieved even for high-molecular-weight PLA through concentration optimization.

Overall, the results of this study demonstrate that nanoprecipitation gives PLA nanoparticles as small as 58 nm at low polymer concentrations. The smallest particles were obtained using acetonitrile as the solvent, PLA with a molecular weight of 170 kDa at a concentration of 0.0625 wt %, and polyvinyl alcohol (PVA) as the surfactant at 1 wt % concentration, which provides steric stabilization of the resulting dispersion. Nanoprecipitation therefore reaches the sub-100 nm range with uniform PLA particles, which is the range of interest for biomedical applications.

Conclusion

The synthesis of polylactide and poly(lactide-*co*-glycolide) nanoparticles by nanoprecipitation was optimized here with a view to PLA-based nanocarriers for neutron capture therapy.

Five factors controlling nanoparticle size and morphology were examined, namely, the type of water-miscible solvent, the polymer molecular weight, the polymer concentration, the organic-to-aqueous phase ratio, and the nature of the surfactant. The use of acetonitrile enabled the production of ultrasmall PLA nanoparticles with sizes as low as 58 nm, even from high-molecular-weight polymers (>100 kDa). Acetonitrile was the most efficient solvent at the lower molecular weights, while from about 170 kDa upwards 1,4-dioxane restrained the growth of the particles most effectively; the partially water-miscible ethyl acetate gave micrometer-sized particles. Sizes of this order are typical of PLGA systems but have not been reported for

PLA of such high molecular weight, which is characterized by greater hydrophobicity and hydrolytic stability. Within the range studied (10–50 vol %), the organic-to-aqueous phase ratio left the particle diameter unchanged.

The smallest of the obtained nanoparticles fall within the 10–100 nm range, which is generally regarded as favorable for overcoming biological barriers and accumulating in tumor tissue via the enhanced permeability and retention effect. The potentially high resistance of high-molecular-weight PLA to hydrolysis makes these systems particularly promising for NCT.

The methods and structure–size relationships reported here are a starting point for further work on the encapsulation of boron-containing compounds and on the surface functionalization of PLA-based nanocarriers for targeted delivery in the neutron capture therapy of cancer.

Experimental

Polylactide (PLA) with molecular weights of 44, 111, 170, 330, and 442 kDa, as well as a copolymer of polylactide and glycolide (PLGA50/50), were purchased from Novokhim, Russia. The molecular weight and dispersity of every batch were determined independently (Table 4), and the values quoted throughout this work are the measured weight-average molecular weights of the polymers themselves. The organic solvents, such as tetrahydrofuran, acetonitrile, acetone, dioxane, and ethyl acetate, were purchased from Component-Reactive, Russia. Surfactants used in the study were polyvinyl alcohol with a molecular weight of 99 kDa (Sigma-Aldrich, USA), Pluronic F-127 (Sigma-Aldrich, USA), Tween 80 (NeoFroxx, Germany), and sodium dodecyl sulfate (Lenreactive, Russia).

Table 4: Measured characteristics of the polymers used, compared with the supplier designation.

Supplier designation	M_w, kDa	M_n, kDa	Dispersity Đ
PLA 44	44	20	2.2
PLA 111	111	51	2.2
PLA 170	170	85	2.0
PLA 330	330	150	2.2
PLA 442	442	215	2.0
PLGA 50/50 41	41	20	2.0
PLGA 50/50 94	94	49	1.9
PLGA 50/50 178	178	92	1.9

Polymeric nanoparticles were synthesized using the nanoprecipitation and emulsion methods. Polymer solutions were prepared at room temperature and used after complete dissolution, judged by the absence of visible gel or undissolved material. The polymer solution (PLA or PLGA) in an organic solvent was added dropwise to an aqueous solution of the surfactant (typically PVA) placed in a 50 mL glass beaker and stirred at 1500 rpm with an IKA RCT basic magnetic stirrer (IKA-Werke, Staufen, Germany) at room temperature. Unless stated otherwise, 2.5 mL of the polymer solution was added to 25 mL of the aqueous phase at a rate of approximately 50 µL per 10 s, that is over about 8 min in total; this corresponds to an organic-phase proportion of 10 vol %, quoted throughout relative to the volume of the aqueous phase. After the addition was complete, the mixture was stirred for a further 24 h in an open vessel at room temperature to complete precipitation and to allow the bulk of the organic solvent to evaporate. The resulting nanoparticles were separated by centrifugation (20,000*g*, 30 min) and washed three times with distilled water (decantation of the supernatant, addition of water, redispersion, and repeated centrifugation) to remove excess surfactant and residual solvent. All size and zeta-potential data reported below refer to the washed dispersions after redispersion in distilled water. The size of the nanoparticles was analyzed using dynamic light scattering (DLS) and scanning electron microscopy (SEM).

Different solvents (acetonitrile, acetone, THF, and dioxane) and polymers with varying molecular weights (44, 111, 170, 330, and 442 kDa) were used to study their impact on nanoparticle size. The polymer concentration was varied from 0.0625 to 1 wt %, and the proportion of the organic phase was varied from 10 to 50 vol % to evaluate their effects on particle size. Different surfactants (PVA, Pluronic F-127, Tween 80, SDS) were tested at concentrations ranging from 0 to 1 wt % to determine their influence on nanoparticle size and stability.

Molecular weights and dispersities were determined by size-exclusion chromatography using a Knauer liquid chromatograph (Germany) equipped with an isocratic pump (1.0 mL·min^{-1}) and a refractive index detector. Measurements were carried out at 40 °C using THF as the eluent. Agilent PLgel columns (particle size 5 µm, pore sizes 10^3 and 10^4 Å) were employed, and the system was calibrated with narrow-dispersity standards. The calibration was verified on polylactide samples of known molecular weight, and the values obtained for all polymers used here agreed with the manufacturer's specifications within the experimental uncertainty; the molecular weights reported in Table 4 are therefore those of the polymers themselves.

Dynamic light scattering experiments were conducted using a Litesizer 500 (Anton Paar GmbH, Graz, Austria). The data acquisition parameters were set as follows: analysis time of 3 min (average of three measurements of 1 min each), scattering angle of 90°, and a temperature of 25 °C. The dispersions were diluted with distilled water before measurement; the

refractive index and viscosity of the dispersant were taken as 1.330 and 0.8872 mPa·s and the refractive index of the particles as 1.46. The diameters quoted are intensity-weighted mean hydrodynamic diameters obtained from cumulant analysis, and the polydispersity index (PDI) is the corresponding cumulant value. Electrophoretic measurements were carried out on the same samples in distilled water, and zeta potentials were calculated from the measured electrophoretic mobility using the Smoluchowski approximation.

Micrometer-sized particles were imaged with a JEOL JSM-6380LA scanning electron microscope (Tokyo, Japan) at an accelerating voltage of 10 kV in secondary-electron mode. Images of the nanoparticles were acquired on a TESCAN MIRA field-emission scanning electron microscope (TESCAN, Brno, Czech Republic) at an accelerating voltage of 3–5 kV in secondary-electron (Everhart–Thornley) mode. Samples were prepared by depositing the dispersion onto a metal stub and drying in air.

All experiments were performed in triplicate (three independent preparations). Data are presented as mean values ± standard deviation. Differences were assessed using Student's t-test and were regarded as significant at $p < 0.05$; differences described in the text as lying within the experimental scatter did not reach this level.

Acknowledgements

Characterization of the samples described in this study was performed using the equipment of Collaborative Access Center "Center for Polymer Research" of ISPM RAS.

Funding

This work was supported by the Ministry of Science and Higher Education of the Russian Federation (agreement no. FFSM-2025-0003).

Author Contributions

Vladislav Potseleev: formal analysis; investigation; methodology; writing – original draft. Artem Kondratenko: formal analysis; investigation; visualization; writing – review & editing. Eugene Statnik: formal analysis; methodology; software; writing – review & editing. Anna Druzina: resources; validation; writing – review & editing. Sergey Uspenskii: funding acquisition; project administration; resources; supervision; writing – review & editing.

ORCID® iDs

Anna Druzina - https://orcid.org/0000-0002-2368-4148
Sergey Uspenskii - https://orcid.org/0000-0002-4134-4622

Data Availability Statement

Data generated and analyzed during this study is available from the corresponding author upon reasonable request.

References

1. Sauerwein, W. A. G.; Wittig, A.; Moss, R.; Nakagawa, Y., Eds. *Neutron Capture Therapy: Principles and Applications;* Springer: Berlin, Germany, 2012. doi:10.1007/978-3-642-31334-9
2. Wu, F.; Sun, P.; Guo, X.; Zhang, Y.; Meng, X.; Li, X.; Li, J.; Chen, N.; Pei, P. *Acta Biomater.* **2025,** *203,* 78–93. doi:10.1016/j.actbio.2025.07.009
3. Taskaeva, I.; Kasatova, A.; Surodin, D.; Bgatova, N.; Taskaev, S. *Life* **2023,** *13,* 518. doi:10.3390/life13020518
4. Deng, S.; Gigliobianco, M. R.; Censi, R.; Di Martino, P. *Nanomaterials* **2020,** *10,* 847. doi:10.3390/nano10050847
5. Bollhorst, T.; Rezwan, K.; Maas, M. *Chem. Soc. Rev.* **2017,** *46,* 2091–2126. doi:10.1039/c6cs00632a
6. Potseleev, V. V.; Trofimchuk, E. S.; Nikonorova, N. I. *Mendeleev Commun.* **2021,** *31,* 515–516. doi:10.1016/j.mencom.2021.07.026
7. Trofimchuk, E. S.; Potseleev, V. V.; Khavpachev, M. A.; Moskvina, M. A.; Nikonorova, N. I. *Polym. Sci., Ser. C* **2021,** *63,* 199–218. doi:10.1134/s1811238221020107
8. Kowalczuk, A.; Trzcinska, R.; Trzebicka, B.; Müller, A. H. E.; Dworak, A.; Tsvetanov, C. B. *Prog. Polym. Sci.* **2014,** *39,* 43–86. doi:10.1016/j.progpolymsci.2013.10.004
9. Vrignaud, S.; Benoit, J.-P.; Saulnier, P. *Biomaterials* **2011,** *32,* 8593–8604. doi:10.1016/j.biomaterials.2011.07.057
10. Malouff, T. D.; Seneviratne, D. S.; Ebner, D. K.; Stross, W. C.; Waddle, M. R.; Trifiletti, D. M.; Krishnan, S. *Front. Oncol.* **2021,** *11,* 601820. doi:10.3389/fonc.2021.601820
11. Tyler, B.; Gullotti, D.; Mangraviti, A.; Utsuki, T.; Brem, H. *Adv. Drug Delivery Rev.* **2016,** *107,* 163–175. doi:10.1016/j.addr.2016.06.018
12. Ramot, Y.; Haim-Zada, M.; Domb, A. J.; Nyska, A. *Adv. Drug Delivery Rev.* **2016,** *107,* 153–162. doi:10.1016/j.addr.2016.03.012
13. Khavpachev, M. A.; Trofimchuk, E. S.; Nikonorova, N. I.; Garina, E. S.; Moskvina, M. A.; Efimov, A. V.; Demina, V. A.; Bakirov, A. V.; Sedush, N. G.; Potseleev, V. V.; Cherdyntseva, T. A.; Chvalun, S. N. *Macromol. Mater. Eng.* **2020,** *305,* 2000163. doi:10.1002/mame.202000163
14. Trofimchuk, E. S.; Moskvina, M. A.; Ivanova, O. A.; Potseleev, V. V.; Demina, V. A.; Nikonorova, N. I.; Bakirov, A. V.; Sedush, N. G.; Chvalun, S. N. *Mendeleev Commun.* **2020,** *30,* 171–173. doi:10.1016/j.mencom.2020.03.013
15. Matsumura, Y.; Maeda, H. *Cancer Res.* **1986,** *46,* 6387–6392.
16. Fang, J.; Nakamura, H.; Maeda, H. *Adv. Drug Delivery Rev.* **2011,** *63,* 136–151. doi:10.1016/j.addr.2010.04.009
17. Wilhelm, S.; Tavares, A. J.; Dai, Q.; Ohta, S.; Audet, J.; Dvorak, H. F.; Chan, W. C. W. *Nat. Rev. Mater.* **2016,** *1,* 16014. doi:10.1038/natrevmats.2016.14
18. Marcet, I.; Weng, S.; Sáez-Orviz, S.; Rendueles, M.; Díaz, M. *J. Food Eng.* **2018,** *239,* 26–32. doi:10.1016/j.jfoodeng.2018.06.030
19. Zielińska, A.; Carreiró, F.; Oliveira, A. M.; Neves, A.; Pires, B.; Venkatesh, D. N.; Durazzo, A.; Lucarini, M.; Eder, P.; Silva, A. M.; Santini, A.; Souto, E. B. *Molecules* **2020,** *25,* 3731. doi:10.3390/molecules25163731

20. Pineda-Reyes, A. M.; Hernández Delgado, M.; de la Luz Zambrano-Zaragoza, M.; Leyva-Gómez, G.; Mendoza-Muñoz, N.; Quintanar-Guerrero, D. *RSC Adv.* **2021,** *11,* 2226–2234. doi:10.1039/d0ra07749f
21. Vu, K. B.; Phung, T. K.; Tran, T. T. T.; Mugemana, C.; Giang, H. N.; Nhi, T. L. P. *J. Ind. Eng. Chem. (Amsterdam, Neth.)* **2021,** *97,* 307–315. doi:10.1016/j.jiec.2021.02.010
22. Perevyazko, I.; Vollrath, A.; Hornig, S.; Pavlov, G. M.; Schubert, U. S. *J. Polym. Sci., Part A: Polym. Chem.* **2010,** *48,* 3924–3931. doi:10.1002/pola.24157
23. Perevyazko, I. Y.; Vollrath, A.; Pietsch, C.; Schubert, S.; Pavlov, G. M.; Schubert, U. S. *J. Polym. Sci., Part A: Polym. Chem.* **2012,** *50,* 2906–2913. doi:10.1002/pola.26071
24. El-Shabouri, M. H. *Int. J. Pharm.* **2002,** *249,* 101–108. doi:10.1016/s0378-5173(02)00461-1
25. Brunel, F.; Véron, L.; David, L.; Domard, A.; Delair, T. *Langmuir* **2008,** *24,* 11370–11377. doi:10.1021/la801917a
26. Yoksan, R.; Jirawutthiwongchai, J.; Arpo, K. *Colloids Surf., B* **2010,** *76,* 292–297. doi:10.1016/j.colsurfb.2009.11.007
27. Kafshgari, M. H.; Khorram, M.; Mansouri, M.; Samimi, A.; Osfouri, S. *Iran. Polym. J.* **2012,** *21,* 99–107. doi:10.1007/s13726-011-0010-1
28. Van Bavel, N.; Lewrenz, A.-M.; Issler, T.; Pang, L.; Anikovskiy, M.; Prenner, E. J. *Polymers (Basel, Switz.)* **2023,** *15,* 1319. doi:10.3390/polym15051319
29. Paques, J. P.; van der Linden, E.; van Rijn, C. J. M.; Sagis, L. M. C. *Food Hydrocolloids* **2013,** *31,* 428–434. doi:10.1016/j.foodhyd.2012.11.012
30. Badri, W.; Miladi, K.; Nazari, Q. A.; Fessi, H.; Elaissari, A. *Colloids Surf., A* **2017,** *516,* 238–244. doi:10.1016/j.colsurfa.2016.12.029
31. Iqbal, M.; Valour, J.-P.; Fessi, H.; Elaissari, A. *Colloid Polym. Sci.* **2015,** *293,* 861–873. doi:10.1007/s00396-014-3464-9
32. Mahmoud, B. S.; McConville, C. *Pharmaceutics* **2021,** *13,* 541. doi:10.3390/pharmaceutics13040541
33. Byun, Y.; Hwang, J. B.; Bang, S. H.; Darby, D.; Cooksey, K.; Dawson, P. L.; Park, H. J.; Whiteside, S. *LWT-Food Sci. Technol.* **2011,** *44,* 24–28. doi:10.1016/j.lwt.2010.06.032
34. Varga, N.; Hornok, V.; Janovák, L.; Dékány, I.; Csapó, E. *Colloids Surf., B* **2019,** *176,* 212–218. doi:10.1016/j.colsurfb.2019.01.012
35. Astete, C. E.; Sabliov, C. M. *J. Biomater. Sci., Polym. Ed.* **2006,** *17,* 247–289. doi:10.1163/156856206775997322
36. Huang, W.; Zhang, C. *Biotechnol. J.* **2018,** *13,* 1700203. doi:10.1002/biot.201700203
37. Govender, T.; Stolnik, S.; Garnett, M. C.; Illum, L.; Davis, S. S. *J. Controlled Release* **1999,** *57,* 171–185. doi:10.1016/s0168-3659(98)00116-3
38. Bivas-Benita, M.; Romeijn, S.; Junginger, H. E.; Borchard, G. *Eur. J. Pharm. Biopharm.* **2004,** *58,* 1–6. doi:10.1016/j.ejpb.2004.03.008
39. Musumeci, T.; Ventura, C. A.; Giannone, I.; Ruozi, B.; Montenegro, L.; Pignatello, R.; Puglisi, G. *Int. J. Pharm.* **2006,** *325,* 172–179. doi:10.1016/j.ijpharm.2006.06.023
40. Hernández-Giottonini, K. Y.; Rodríguez-Córdova, R. J.; Gutiérrez-Valenzuela, C. A.; Peñuñuri-Miranda, O.; Zavala-Rivera, P.; Guerrero-Germán, P.; Lucero-Acuña, A. *RSC Adv.* **2020,** *10,* 4218–4231. doi:10.1039/c9ra10857b
41. Zhang, X.; Luo, Q.; Zhang, F.; Zhao, X.; Li, Y.; Yang, N.; Feng, L. *Molecules* **2024,** *29,* 5566. doi:10.3390/molecules29235566
42. Thauvin, C.; Schwarz, B.; Delie, F.; Allémann, E. *Int. J. Pharm.* **2018,** *548,* 771–777. doi:10.1016/j.ijpharm.2017.11.001
43. Lepeltier, E.; Bourgaux, C.; Couvreur, P. *Adv. Drug Delivery Rev.* **2014,** *71,* 86–97. doi:10.1016/j.addr.2013.12.009
44. Fessi, H.; Puisieux, F.; Devissaguet, J. P.; Ammoury, N.; Benita, S. *Int. J. Pharm.* **1989,** *55,* R1–R4. doi:10.1016/0378-5173(89)90281-0
45. Vitale, S. A.; Katz, J. L. *Langmuir* **2003,** *19,* 4105–4110. doi:10.1021/la026842o
46. Aubry, J.; Ganachaud, F.; Cohen Addad, J.-P.; Cabane, B. *Langmuir* **2009,** *25,* 1970–1979. doi:10.1021/la803000e
47. Simonutti, R.; Bertani, D.; Marotta, R.; Ferrario, S.; Manzone, D.; Mauri, M.; Gregori, M.; Orlando, A.; Masserini, M. *Polymer* **2021,** *218,* 123511. doi:10.1016/j.polymer.2021.123511
48. Beck-Broichsitter, M.; Nicolas, J.; Couvreur, P. *Nanoscale* **2015,** *7,* 9215–9221. doi:10.1039/c5nr01695a
49. Smallwood, I. M. *Handbook of Organic Solvent Properties;* Elsevier: Amsterdam, Netherlands, 1996. doi:10.1016/c2009-0-23646-4
50. Song, K. C.; Lee, H. S.; Choung, I. Y.; Cho, K. I.; Ahn, Y.; Choi, E. J. *Colloids Surf., A* **2006,** *276,* 162–167. doi:10.1016/j.colsurfa.2005.10.064
51. Ruiz, E.; Orozco, V. H.; Hoyos, L. M.; Giraldo, L. F. *Eur. Polym. J.* **2022,** *173,* 111307. doi:10.1016/j.eurpolymj.2022.111307
52. Potseleev, V.; Uspenskii, S.; Kovtun, I.; Sedush, N. *Polymers (Basel, Switz.)* **2026,** *18,* 497. doi:10.3390/polym18040497
53. Ghitman, J.; Stan, R. L. *Mater. Plast. (Bucharest, Rom.)* **2019,** *56,* 857–864. doi:10.37358/mp.19.4.5277
54. Nascimento, M. H. M.; Franco, M. K. K. D.; Yokaichyia, F.; de Paula, E.; Lombello, C. B.; de Araujo, D. R. *Int. J. Biol. Macromol.* **2018,** *111,* 1245–1254. doi:10.1016/j.ijbiomac.2018.01.064
55. Saengsorn, K.; Jimtaisong, A. *Asian Pac. J. Trop. Biomed.* **2017,** *7,* 1092–1096. doi:10.1016/j.apjtb.2017.10.011
56. Miraglia, D. B.; Rodríguez, J. L.; Minardi, R. M.; Schulz, P. C. *J. Surfactants Deterg.* **2011,** *14,* 401–408. doi:10.1007/s11743-010-1239-y
57. Kunieda, H.; Hanno, K.; Yamaguchi, S.; Shinoda, K. *J. Colloid Interface Sci.* **1985,** *107,* 129–137. doi:10.1016/0021-9797(85)90156-0

License and Terms

This is an open access article licensed under the terms of the Beilstein-Institut Open Access License Agreement (https://www.beilstein-journals.org/bjnano/terms), which is identical to the Creative Commons Attribution 4.0 International License (https://creativecommons.org/licenses/by/4.0). The reuse of material under this license requires that the author(s), source and license are credited. Third-party material in this article could be subject to other licenses (typically indicated in the credit line), and in this case, users are required to obtain permission from the license holder to reuse the material.

The definitive version of this article is the electronic one which can be found at:
https://doi.org/10.3762/bjnano.17.111